University of HUDDERSFIELD

University of Huddersfield Repository

Gu, Fengshou, Tian, Xiange, Chen, Zhi, Wang, Tie, Rehab, Ibrahim and Ball, Andrew

Fault severity diagnosis of rolling element bearings based on kurtogram and envelope analysis

Original Citation

Gu, Fengshou, Tian, Xiange, Chen, Zhi, Wang, Tie, Rehab, Ibrahim and Ball, Andrew (2014) Fault severity diagnosis of rolling element bearings based on kurtogram and envelope analysis. In: Proceedings of the International conference on advances in civil, Structural and Mechanical Engineering. Institute of Research Engineers and Doctors. ISBN 978-981-07-8859-9

This version is available at https://eprints.hud.ac.uk/id/eprint/21118/

The University Repository is a digital collection of the research output of the University, available on Open Access. Copyright and Moral Rights for the items on this site are retained by the individual author and/or other copyright owners. Users may access full items free of charge; copies of full text items generally can be reproduced, displayed or performed and given to third parties in any format or medium for personal research or study, educational or not-for-profit purposes without prior permission or charge, provided:

- The authors, title and full bibliographic details is credited in any copy;
- A hyperlink and/or URL is included for the original metadata page; and
- The content is not changed in any way.

For more information, including our policy and submission procedure, please contact the Repository Team at: E.mailbox@hud.ac.uk.

http://eprints.hud.ac.uk/

Fault severity diagnosis of rolling element bearings based on kurtogram and envelope analysis

Fengshou Gu, Xiange Tian, Zhi Chen, Tie Wang, Ibrahim Rehab and Andrew Ball

***Abstract*— Faults in rolling element bearing are among the main causes of breakdown in rotating machines. Vibration is an effective technique for machine condition monitoring. Vibration signals from a defective bearing with a localized fault contain a series of impulsive responses, which result from the impacts of the defective part(s) with other elements. Most researches carried out have focused on fault location identification. However, limited work has been reported for fault severity estimation, which is critical to make decision for maintenance actions. To improve current diagnostic capability, this paper pays more attention to bearing fault severity diagnosis. It models the vibration sources from bearing defects as an impact process with constant size but three different lengths corresponding to outer race fault, inner race fault and roller fault, respectively. Then an experimental study was followed to evaluate this model. Moreover, the conventional envelope analysis of the measured vibration signals from the tested faulty bearings is optimized by spectral kurtosis (SK) for automatic and reliable fault detection and fault category diagnosis. In the meantime, the diagnostic parameters for fault severity estimation: root mean squared (RMS) values and kurtosis amplitude are developed based on the model results and subsequently evaluated to be agreed vigorously with tested fault cases.**

***Keywords*—kurtogram, envelope analysis, bearing fault diagnosis, elastic deformation, geometry deformation**

I. Introduction

Rolling element bearings are key components in modern machinery. Detection and diagnosis of their faults are very important, as it prevents any further deterioration of other components which may lead to catastrophic failures. For a clear diagnosis of the bearing fault, a number of techniques have been proposed to separate deterministic components from the bearing component. Darlow explored high frequency resonance technique (HFRT), which is also widely known as envelope analysis [1]. Antoni applied cyclostationary spectral analysis to fault detection and diagnosis in rolling element bearings [2, 3]. Furthermore, cepstrum analysis, bispectrum analysis and time-frequency analysis are also introduced to bearing fault diagnostic. D. Ho and R.B. Randall investigated the efficient application of self-adaptive noise cancellation (SANC) in conjunction with envelope analysis in order to remove discrete frequency masking in bearing vibration signals [4]. Barszcz applied SANC to denoise wind turbines vibration signal for outer race fault diagnosis [5]. N. Sawalhi, R. B. Randall and H. Endo presented an algorithm for enhancing the surveillance capability of SK by using the minimum entropy deconvolution (MED) technique. The MED technique effectively deconvolves the effect of the transmission path and clarifies the impulses, even where they are not separated in the original signal [6]. S. Zhao applied empirical mode decomposition (EMD) and the Approximate Entropy (ApEn) method for quantitative diagnosis of a spall-like fault of a rolling element bearing [7]. Barszcz proposed a new method named protrugram, which is based on the kurtosis of the envelope spectrum amplitudes of the demodulated signal, rather than on the kurtosis of the filtered time signal. The advantage of the method is the ability to detect transients with smaller signal-to-noise ratio (SNR) comparing to the SK based kurtogram [8].

However, most of these works are for fault detection and fault type diagnosis and limited investigations are on fault severity estimation, which is critical to make decisions for maintenance actions. To improve current diagnostic capability, this paper pays more attention to bearing fault severity diagnosis.

Fengshou Gu, Xiange Tian, Ibrahim Rehab and Andrew Ball
University of Huddersfield
UK
F.Gu@hud.ac.uk, u1178848@hud.ac.uk

Zhi Chen, Tie Wang
Taiyuan University of Technology
P.R. China

II. Characteristic frequencies of bearing faults

Rolling element bearing consists of an inner race, an outer race, rolling elements and a cage, which holds the rolling elements in a given relative position, as presented in Fig. 1. In order to find the characteristics of the vibration responses due to faults, the bearing rings are assumed to be isolated continuous systems. It is further assumed that: (1) All rollers are equal in diameter; (2) There is in pure rolling contact between rollers, inner race and outer race; (3) There is no slipping between the shaft and the bearing; (4) Outer race is

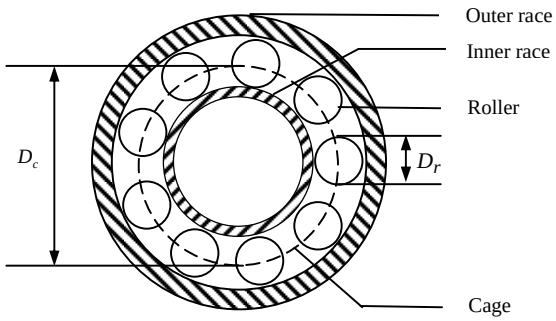

Figure 1. Rolling element bearing components

stationary and inner race rotates. The relative velocity between rollers, inner race and outer race are zero because they are in pure rolling contact.

Race surface fatigue results in the appearance of spalls on the inner race, outer race or rolling elements. If one of the races has a spall, it will almost periodically impact with rolling elements. The fault signature is represented by successive impulses with a repetition rate depending on the faulty component, geometric dimensions and the rotational speed. The period between impacts is different for all the listed elements and depends on the geometry of the bearing, the rotational speed and the load angle. For a fixed outer race bearing, the theoretical characteristic fault frequencies can be calculated using (1)-(4), and a derivation of these equations is presented in [9].

Fundamental cage frequency:

$$F_C = \frac{1}{2} F_s (1 - \frac{D_r}{D_c} \cos\phi) \quad (1)$$

Outer race defect frequency:

$$F_{RPO} = \frac{N_r}{2} F_s (1 - \frac{D_r}{D_c} \cos\phi) \quad (2)$$

Inner race defect frequency:

$$F_{RPI} = \frac{N_r}{2} F_s (1 + \frac{D_r}{D_c} \cos\phi) \quad (3)$$

Roller defect frequency:

$$F_{RS} = \frac{D_c F_s}{2 D_r} (1 - \frac{D_r^2}{D_c^2} \cos^2\phi) \quad (4)$$

where, D_c is pitch circle diameter, D_r is roller diameter, ϕ is contact angle, N_r is number of roller and F_s is shaft rotational frequency.

In practice there is always slight sliding and slippage, especially when a bearing is under dynamic loads and with severe wear. Therefore, these frequencies may have a slight difference from calculated ones above.

III. Vibration responses to different sizes of fault

The bearing frequency equations provide a theoretical estimate of the frequencies to be expected when various defects occur on the bearing elements, based upon the assumption that an ideal impulse will be generated whenever a bearing element encounters the defect. For localised bearing faults such as spalling and pitting, sharp force impacts will be generated. These impacts will excite structural resonances and the resulting vibration will be measured by the transducer mounted externally on the machine casing [10].

However, due to the different geometry of the contact between the localised fault and the bearing component, the contact-stiffness can change because of the different geometrical properties in contact zones. On the other hand, a damaged bearing (particularly a small damage at an early stage of damage development) usually produces small amplitudes of vibration in high frequency bands due to impulsive impacts[11].

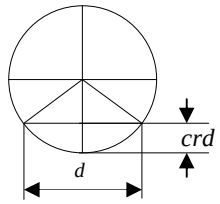

Figure 2. Schematic diagram of geometry deformation

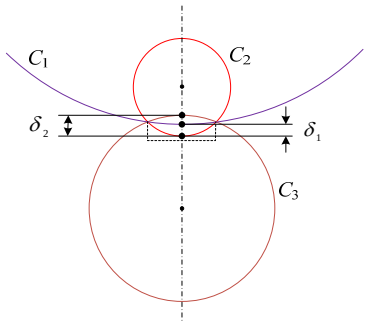

Figure 3. Geometry deformation for two kinds of contact

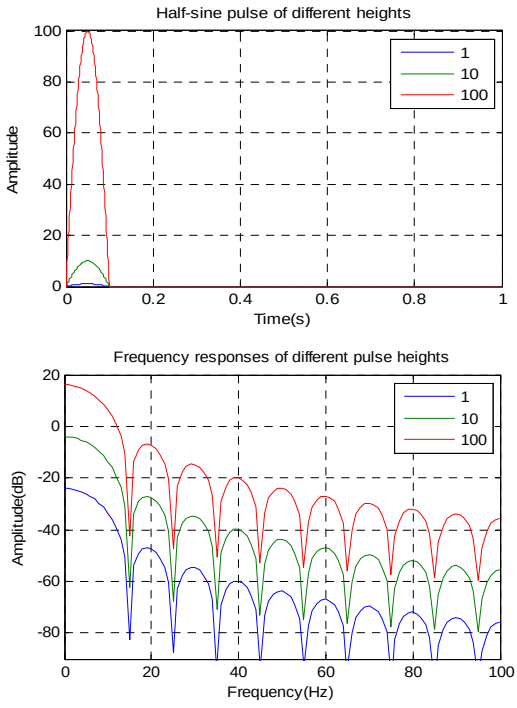

Figure 4. Frequency responses of difference pulse heights

The contact deformation is composed of geometric deformation and elastic deformation. Elastic deformation occurs along the contact surfaces of a bearing's rolling elements and raceway surfaces under loading. Geometric deformation caused by defect is related to defect location and size. While elastic deformation is related to load and defect size.

The total deformation Δ includes geometry deformation δ_g and elastic deformation δ_e.

$$\Delta = \delta_g + \delta_e \tag{5}$$

As shown in Fig. 2, if the width of fault is d and radius of circle is r, the chord height can be expressed as

$$crd = r - \sqrt{r^2 - \left(\frac{d}{2}\right)^2} \ . \tag{6}$$

There are two kinds of contact model between bearing components as shown in Fig. 3, which are contact between a convex and a concave surface (C1 and C2) and contact between two convex surfaces (C2 and C3). If the chord height for C1, C2 and C3 are defined as $crd1$, $crd2$ and $crd3$. The geometry deformation of concave-convex contact δ_1 and concave-concave contact δ_2 are given out by (7) and (8), respectively.

$$\delta_1 = crd2 - crd1 \tag{7}$$

$$\delta_2 = crd2 + crd3 \tag{8}$$

Furthermore, considering that the fault on inner race creates concave-concave contact whereas the fault on the roller has both concave-concave and concave-convex contact. The vibration impact from the inner race defect may create the highest responses when the sizes of the faults are the same over different races. From the relationship it is easy to understand that geometry deformations on different components have a relationship as shown in (9).

$$\delta_{go} < \delta_{gr} < \delta_{gi} \tag{9}$$

Based on this relationship, Fig. 4 illustrates half-sine pulses of three different heights: 1, 10 and 100 and their frequency responses. It is obvious that when the amplitude is higher, the frequency response increases. This shows that when the fault size is the same, the fault on inner race may produce the highest responses whereas the fault on the outer race will cause the lowest responses.

Taking into account the elastic deformation, it is easy to understand the impulsive differences between different fault severities. As fault degree increases, the load area will decrease while elastic deformation δ_e will increase, which will result in the growth of impulse height.

IV. Signal processing based on kurtogram

The envelope spectrum is a very efficient diagnostic tool for the aforementioned faults, as the information about the fault is extracted from the spacing between impulses but not from the excited frequencies. The process of obtaining the envelope spectrum is often named as signal demodulation. However, the quality of the demodulated signal depends on the frequency band selected for the demodulation, which requires two parameters bandwidth and central frequency [12].

SK is a powerful tool for detecting the presence of transients in a signal, even when they are buried in strong additive noise, by indicating in which frequency bands they are taken place. The Kurtogram optimization considers a variety of bandwidths and central frequencies. It is basically a cascade of SK obtained for different values of the Short Time Frequency Transform (STFT) window length.

The SK of the complex envelope $X(t, f)$ can be calculated [12] as,

$$K(f) = \frac{\left\langle \left| X(t, f) \right|^4 \right\rangle}{\left\langle \left| X(t, f) \right|^2 \right\rangle^2} - 2 \tag{10}$$

where the subtraction of 2 is used to enforce $K(f) = 0$ in the case $X(t, f)$ is complex Gaussian (instead of 3 for real signals). Then, equation for kurtogram of a signal based on STFT can be presented as (11),

$$K_x(f, n) = \frac{\left\langle \left| X(t, f)_n \right|^4 \right\rangle}{\left\langle \left| X(t, f)_n \right|^2 \right\rangle^2} - 2 \tag{11}$$

where, n denotes the window length of STFT.

V. Test rig description

The experimental data analysed in this paper was collected from the bearing test rig illustrated in Fig. 5. It is composed of motor, coupling, shaft, bearings and brake.

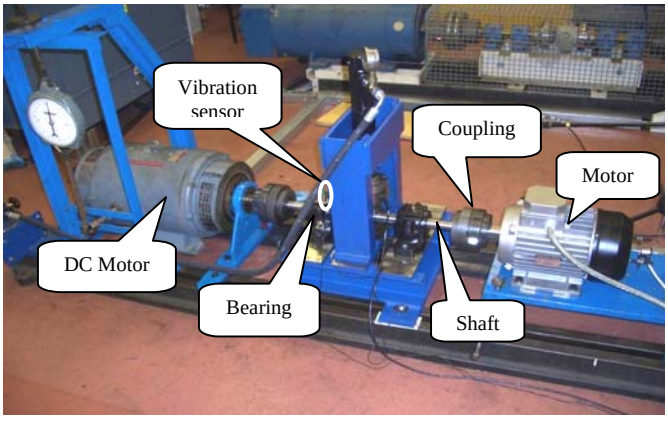

Figure 5. Photo of bearing test rig

Bearing type is NSK N406 cylindrical roller bearing and its geometric dimensions are listed in Table I. One Sinocera piezoelectric accelerometer is mounted on the housing of the N406 bearing vertically to measure the vibration. The frequency range of accelerometer is from 0.5 Hz to 10 kHz and the sensitivity is 8.08 mv/ms^2.

Defect frequencies in experiment calculated according to equation (4)-(9) are listed in Table II.

TABLE I. SPECIFICATION OF NSK TYPE N406 CYLINDRICAL ROLLER BEARING

Parameter	Measurement
Pitch Diameter	59 mm
Bore Diameter	30 mm
Roller Diameter	14 mm
Roller Number	9
Contact Angle	0

TABLE II. FAULT CHARACTERISTIC FREQUENCIES

Fault type	Defect frequency (Hz)
Outer race	85.8
Inner race	139.2
Roller	49.7

Fig. 6 gives out the photo of defect rolling bearing with 30% roller fault, 60% inner race fault and 100% outer race fault, respectively. In experiment, defect was made on roller, inner race and outer race with three different severities (30%, 60% and 100%) on each component, separately.

(a) 30% roller fault (b) 60% inner race fault (c) 100% outer race fault

Figure 6. Photo of fault bearing

VI. Signal processing results and discussion

In this section, experimental data processing results are discussed based on mechanical vibration model. Same baseline signal is applied to outer race, inner race and roller fault for comparison.

Fig. 7 shows raw vibration signals for baseline, inner race and outer race at four kinds of conditions, respectively. It can be seen that the vibration amplitudes of outer race are smaller than inner race and roller for three kinds of fault severities. In the meantime, the vibration amplitude of roller is higher than inner race at 100% damage but similar at both 30% damage and 60% damage.

Fig. 8-10 give out envelope analysis results of three kinds of fault. From the figures, it is obvious that characteristic frequencies and their harmonics are significant , which verifies that filter parameters can be optimised by kurtosis maximum principle effectively.

The amplitude of inner race fault frequency grows with the damage severity while the outer race and roller fault do not have such good trend. Envelope analysis results indicate it can be applied for fault detection and recognise the fault type by fault characteristic frequencies.

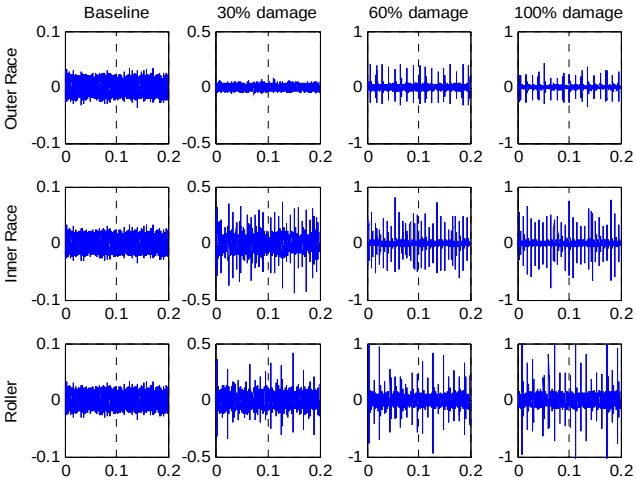

Figure 7. Vibration signals in the time domain

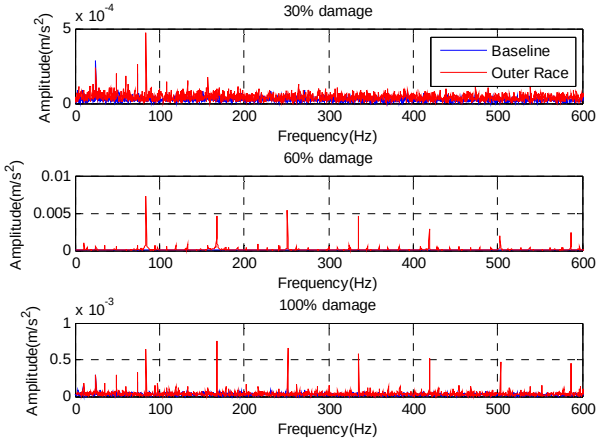

Figure 8. Envelope analysis results for outer race defect

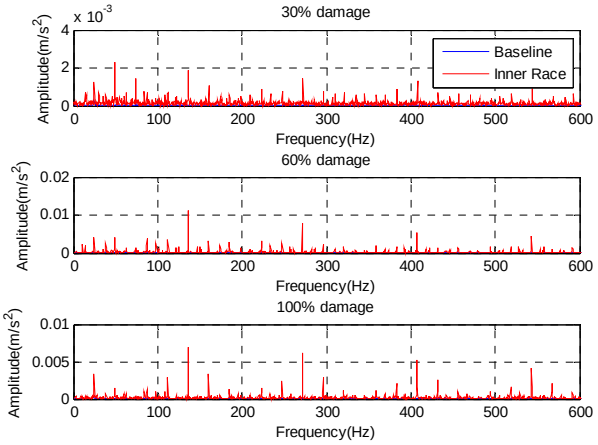

Figure 9. Envelope analysis results for inner race defect

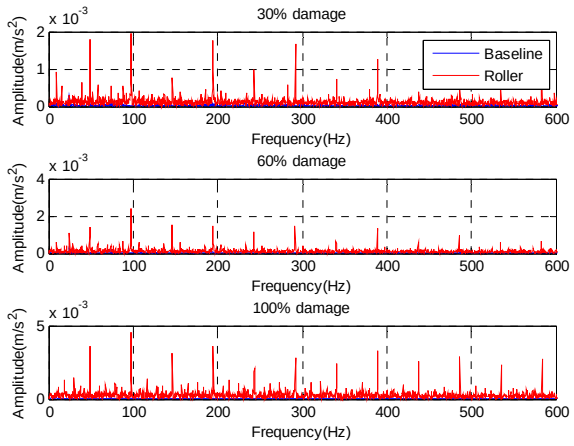

Figure 10. Envelope analysis results for roller defect

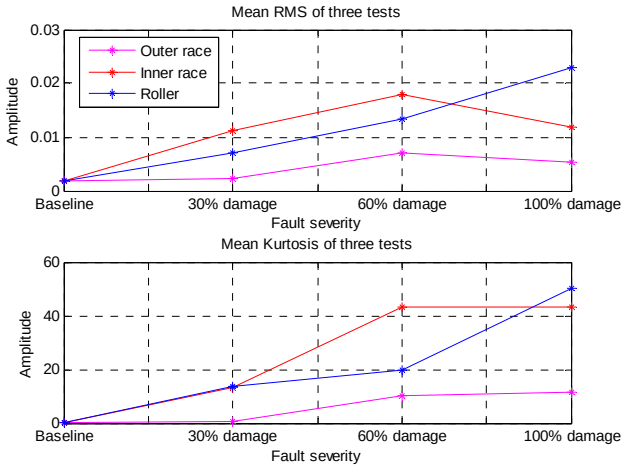

Figure 11. Mean RMS and Kurtosis comparison results

Fig. 11 demonstrates mean RMS and kurtosis comparison of three tests results. RMS value increases greatly with the damage severity and shows obvious difference between three kinds of faults. But 100% damage does not follow the prediction because the motion between bearing components includes slippage. In addition, kurtosis results can also separate outer race fault. However the difference is tiny between inner race and roller fault, showing that the RMS is the better choice for fault diagnosis.

When there is a same size fault on outer race, inner race and roller, the fault impulse amplitude of outer race is constant and smaller and waveform impulse is less spikiness, while the inner race fault frequency is modulated at shaft frequency and roller fault frequency is modulated at cage frequency. With same size on three components separately, the outer race impulse has lowest "peakedness" compared with inner race fault. On the contrary, roller fault has the largest deformation and should have highest "peakedness" which is not reality in experimental results. This may be caused by the high level noises in roller vibration which will impact the kurtosis value.

The experimental data analysis results show that the RMS and kurtosis value can be relied on to predict bearing fault severity, which provides decisive reference for taking maintenance actions.

VII. Conclusion

In this paper, an adaptive filter technique has been developed by combining SK with envelope analysis for rolling bearing fault detection and diagnosis. The adaptive filter is applied to improve SNR. The filter parameters including band width and central frequency are optimised by a maximal SK criterion. Then, the filtered vibration signal is analysed by envelope analysis for fault feature extraction. The effectiveness of the proposed method has been evaluated based on experimental data sets from three types of faults and three levels of damage severities. The diagnostic results show that not only the types of fault can be identified correctly but also the severity is estimated with a good degree of accuracy.

References

[1] M. S. Darlow, R. H. Badgley and G. W. Hogg, "Application of high frequency resonance techniques for bearing diagnostics in helicopter gearboxes," Technical Report, US Army Air Mobility Research and Development Laboratory, 1974, pp.74–77.

[2] J. Antoni, "Cyclic spectral analysis in practice", Mechanical Systems and Signal Processing, vol. 21, 2007, pp.597–630.

[3] J. Antoni, "Cyclostationarity by examples", Mechanical Systems and Signal Processing, vol. 23, 2009, pp.987–1036.

[4] D. Ho and R. B. Randall, "Optimisation of bearing diagnostic techniques using simulated and actual bearing fault signals", Mechanical Systems and Signal Processing, vol. 14(5), 2000, pp.763-788.

[5] T. Barszcz, "Decomposition of vibration signals into deterministic and nondeterministic components and its capabilities for fault detection and identification", International Journal of Applied Mathematics and Computer Science, vol. 19, 2009, pp.327-335, ISSN (Print) 1641-876X.

[6] N. Sawalhi, R. B. Randall and H. Endo, "The enhancement of fault detection and diagnosis in rolling element bearings using minimum entropy deconvolution combined with spectral kurtosis", Mechanical Systems and Signal Processing, vol. 21, 2007, pp.2616–2633.

[7] S. Zhao, L. Liang, G. Xu, J. Wang and W. Zhang, "Quantitative diagnosis of a spall-like fault of a rolling element bearing by empirical mode decomposition and the approximate entropy method", Mechanical Systems and Signal Processing, vol. 40, 2013, pp.154–177.

[8] T. Barszcz and A. Jablonski, "A novel method for the optimal band selection for vibration signal demodulation and comparison with the Kurtogram", Mechanical Systems and Signal Processing, vol. 25, 2011, pp.431–451.

[9] Tomasz Barszcz and Nader Sawalhi, "Fault Detection Enhancement in Rolling Element Bearings Using the Minimum Entropy Deconvolution", Archives of Acoustics, vol. 37, 2012, pp.131-141.

[10] T. Igarashi and H. Hamada, "Studies on the vibration and sound of defective rolling bearings (First Report: Vibration of Ball Bearings with One Defect)", Bulletin of the Japan Society of Mechanical Engineers, vol. 25, 1982, pp.621-822.

[11] N. Tandon and A. Choudtury, "An analytical model for the prediction of the vibration response of rolling element bearings due to a localized defect", Journal of Sound and Vibration, vol. 205(3), 1997, pp. 275-292.

[12] R. B. Randall and J. Antoni, "Rolling element bearing diagnostics – A tutorial", Mechanical Systems and Signal Processing, vol. 25, 2011, pp.485–520.